Proton and metal binding by cyclen-based highly rigid cryptands†

Carla Bazzicalupi,[a] Andrea Bencini,*[a] Samuele Ciattini,[a] Franck Denat,*[b] Pauline Désogère,[b] Christine Goze,[b] Irene Matera[a] and Barbara Valtancoli[a]

Received 3rd August 2010, Accepted 15th September 2010
DOI: 10.1039/c0dt00948b

The basicity properties of the two cryptands L1 and L2, featuring, respectively, a dibenzofuran or a diphenyl ether moiety bridging the 1,7 positions of a 1,4,7,10-tetraazacyclododecane macrocycle (cyclen) have been studied by means of potentiometric, UV-vis and fluorescence emission measurements. Both ligands show a high basicity in the first protonation step, the first basicity constant of L1 being too high to be measured in aqueous solution. The crystal structure of $\{[HL1]L1\}^+$ shows that the NH_2^+ group is involved in an intramolecular hydrogen bonding network, which justifies the observed high basicity in solution. ^1H, ^{13}C NMR, UV-vis and fluorescence emission measurements show that, among first row divalent metal cations, both L1 and L2 selectively bind in acetonitrile Cu(II) and Zn(II), which are encapsulated within the ligand cavities. Zn(II) coordination is accompanied by a remarkable increase of the fluorescence emission of the ligands, pointing out that the molecular architecture displayed by L1 and L2 can be used to develop new OFF/ON chemosensors for this metal cation.

Introduction

Polyamine macrocycles are undoubtedly versatile receptors for metal cations.[1–24] In fact, depending on their structural features, they can form stable metal chelates in solution and/or act as selective complexing agents for metal cations.[1–6] From this point of view, polyamines are known for their ability to form stable complexes with metal cations of environmental or toxicological relevance, such as Cd(II) or Pb(II) or of biological relevance, such as Cu(II) or Zn(II). Therefore, polyamines represent, in principle, optimal candidates for the assembly of complexing agents for metal cations. On the other hand, polyamines are also double-faced ligands: if they give stable complexes with a variety of metal cations in aqueous solutions, they often present scarce selectivity. For instance, polyamines generally form complexes with Zn(II), Cd(II) and Pb(II) featured by similar stability in aqueous solutions.[1–4] Furthermore, the ability of a polyamine receptor to bind a selected metal cation depends on the characteristics of the medium, such as temperature and pH. In particular, the binding ability of polyamines can be strongly pH-dependent.[7,13–18,22–24] In fact, polyamines can easily protonate in aqueous solution. Protonation of polyamine groups competes with the process of metal complexation and can lead to the formation in solution of protonated metal complexes, where H^+ ions and metal cations in solution are simultaneously bound to the receptors.[13–16]

Structural factors, such as ligand rigidity, type of donor atoms and their disposition, have been shown to play significant roles in determining the binding features of macrocycles toward metal cations, and can be appropriately tuned to improve the selectivity of polyamine receptors. In this context, we have recently inserted heteroaromatic subunits, such as 2,2′-dipyridine, 1,10-phenanthroline, acridine and 2,2′:6′,2″-terpyridine as integral parts of the receptor.[22–24] The rigidity of these units leads to stiffening of the macrocyclic structure giving rise, in some cases, to particular selectivity pattern in metal ion recognition, such as selective Cd(II) coordination over Zn(II) and Pb(II).[22] Furthermore, incorporation of these moieties into macrocyclic structures may allow to combine within the same ligand the special complexation features of macrocycles with the photophysical and photochemical properties displayed by the metal complexes of the heterocycles,[25] resulting in the achievement of polyamine receptors able not only to selectively bind but also to signal selected metal cations thanks to changes of the fluorescence emission of the heteroaromatic units.

A different route to selectively bind targeted metal cations is the use of macrobicyclic receptors featuring highly pre-organized sets of donors and inner cavities of appropriate dimension to encapsulate selected metal cations.[26–31] In particular, small cyclen-based aza-macrobicycles generally feature *endo* configuration of the donor atoms, which determine the formation of highly stable metal complexes. On the other hand, they often possess three-dimensional cavities of small size and their nitrogen donors may behave as very strong bases in aqueous solution, due to the involvement of the H^+ ion in a stabilizing network of intramolecular hydrogen bonds. In some cases small azacryptands behave as "proton sponge", *e.g.*, they cannot be deprotonated in aqueous solution, avoiding or making difficult metal complexation.[32]

Some of us have recently communicated a novel general synthetic route to obtain 1,7-difunctionalized 1,4,7,10-tetraazacyclododecane (cyclen) moieties.[33] This procedure can also be used to achieve cyclen-based cryptands, such as L1 and L2, featuring a dibenzofuran or diphenyl ether unit connecting the nitrogen atoms in 1,7 position of the tetraaza moiety (Scheme 1).[33]

[a]*Dipartimento di Chimica Ugo Schiff, Università di Firenze, Via della Lastruccia 3, 50019, Sesto Fiorentino, Firenze, Italy. E-mail: andrea.bencini@unifi.it*
[b]*Institut de Chimie Moléculaire de l'Université de Bourgogne, UMR CNRS 5260, Université de Bourgogne, 9 avenue Alain Savary, 21078, Dijon, France. E-mail: Franck.Denat@u-bourgogne.fr*

† Electronic supplementary information (ESI) available: Additional data. CCDC reference numbers 787304–787308. For ESI and crystallographic data in CIF or other electronic format see DOI: 10.1039/c0dt00948b

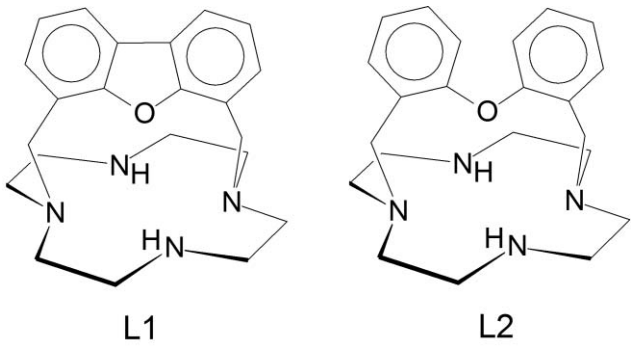

Scheme 1

As our first attempt to use small azacryptands as potential selective binders and fluorescent chemosensors for transition and post-transition metal cations, we have undertaken the study of the protonation and coordination characteristics of L1 and L2 and the results are herein reported.

Results and discussion

Protonation of ligands

Crystal structure of {[HL1]L1}ClO_4·3.5H_2O (a). This compound was isolated in the attempt to obtain the free amine from its triperchlorate salt by treatment with concentrated NaOH aqueous solution and extraction of the aqueous phase with chloroform. Slow evaporation of the organic phase afforded crystals of {[HL1]L1}ClO_4·3.5H_2O. The crystal structure of this compound is constituted by $[HL1]^+$ cations and L1 molecules, coupled *via* hydrogen bonding (Fig. 1), perchlorate anions and water solvent molecules. The ΔF map allowed us to localize five hydrogen atoms on the four secondary nitrogen atoms of two adjacent macrobicycles. As a consequence, the crystal lattice contains couples of L1 molecules and $[HL1]^+$ cations, which strongly interact each other *via* an $NH^+ \cdots N$ hydrogen bond and four C–H $\cdots \pi$ contacts, each involving a C_6-ring of one ligand and a faced hydrogen belonging to methylene group of the other ligand (the distance between the carbon atom of the methylene group and the centroid of the aromatic ring is 3.6 Å) (Fig. 1c). In both L1 and $[HL1]^+$ the N–H bonds pointing inside the cavity give rise to a dense hydrogen bonding network involving the tertiary nitrogen atoms and the oxygen atom of the dibenzofuran unit.

L1 and $[HL1]^+$ display very similar conformations and the overall $\{[HL1]L1\}^+$ adduct possesses a non-crystallographic inversion centre. In fact, in both L1 and $[HL1]^+$ the four nitrogen atoms of the tetraazamacrocycle define a plane (mean deviation *ca.* 0.3 Å) of a square pyramid whose apical position is occupied by the ethereal oxygen, located 2.4 Å apart from the basal plane. The rigid bridging group is asymmetrically bent toward one of the secondary nitrogens. The conformation of the 12-membered tetraazamacrocycle can be described, using the formalism proposed by J. Dale,[34] as [2334]. In this formalism the tetraazamacrocyclic ring is approximately described as a square and the numbers within brackets indicate the number of adjacent bonds constituting each side of the square. The [2334] conformation has been rarely observed in cyclen derivatives,[35] the most common being the more regular [3333] conformation,[35] where each side is constituted by three bonds.

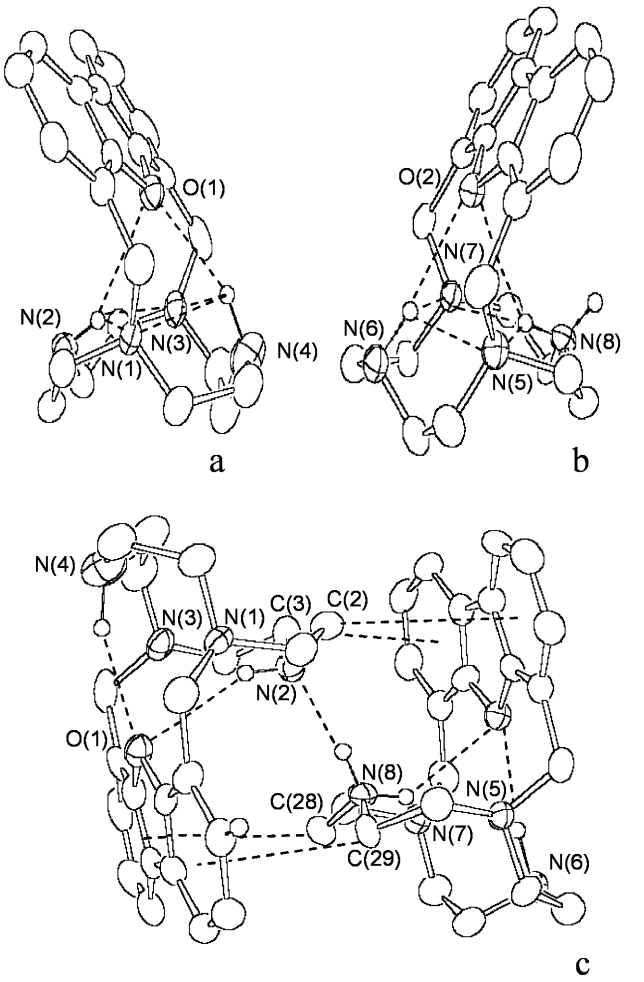

Fig. 1 ORTEP view of L1 (a) and $[HL1]^+$ (b) (thermal ellipsoid plotted at 50% probability level), displaying the intramolecular hydrogen bonding network, and of {[HL1]L1} (c), showing the intermolecular hydrogen bonding interactions in the {[HL1]L1}ClO_4·3.5H_2O compound. Selected hydrogen bonding distances (Å): N(2)–H(4) $\cdots$ N(1) 2.37(6), N(2)–H(4) $\cdots$ N(3) 2.47(7), N(2)–H(4) $\cdots$ O(1) 2.51(7), N(4)–H(5) $\cdots$ N(1) 2.49(1), N(4)–H(5) $\cdots$ N(3) 2.77(8), N(4)–H(5) $\cdots$ O(1) 2.35(4), N(6)–H(1) $\cdots$ N(5) 2.34(6), N(6)–H(1) $\cdots$ N(7) 2.49(6), N(6)–H(1) $\cdots$ O(2) 2.34(2), N(8)–H(2) $\cdots$ N(5) 2.37(6), N(8)–H(2) $\cdots$ N(7) 2.29(7), N(8)–H(2) $\cdots$ O(2) 2.51(7), N(8)–H(3) $\cdots$ N(2) 1.89(8).

Crystal structures of $[H_2L2](ClO_4)_2$ (b) and $[H_2L2]ZnCl_4$·H_2O (c). The crystal structure of $[H_2L2](ClO_4)_2$ (Fig. 2) consists of $[H_2L2]^{2+}$ cations and perchlorate anions. The four nitrogen atoms are in *endo* conformation and define a plane (mean deviation *ca.* 0.05 Å) of a square pyramid whose apical position is occupied by the O(1) oxygen (2.3 Å apart from the basal plane). The phenyl rings are not co-planar, forming a dihedral angle of 67°.

Although the hydrogen atoms of the NH_2^+ groups were not localized in the ΔF map, both the secondary nitrogen atoms are at a short distance from one oxygen of the perchlorate anions and the oxygen of diphenyl ether; this suggests that the H^+ ions are localized on the secondary nitrogen atoms, giving rise to intermolecular hydrogen bonds with perchlorate oxygen atoms

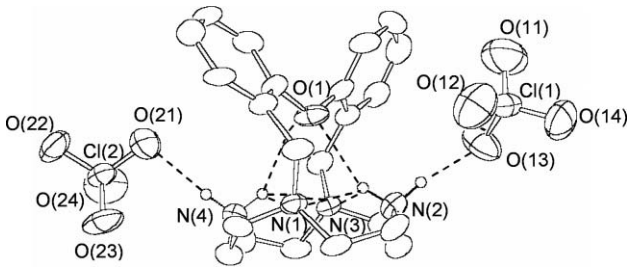

Fig. 2 ORTEP view of the $[H_2L2](ClO_4)_2$ compound (thermal ellipsoid plotted at 50% probability level). Hydrogen bonding distances (Å): N(1)···N(2) 2.772(7), N(1)···N(4) 2.867(7), N(2)···N(3) 2.899(7), N(2)···O(1) 3.130(7), N(2)···O(13) 2.909(8), N(4)···N(3) 2.752(7), N(4)···O(1) 3.231(7), N(4)···O(21) 2.935(9).

and intramolecular hydrogen bonding contacts with the ethereal oxygen and the bridgehead tertiary nitrogen atoms.

The overall conformation of the ligand in its diprotonated cation is characterized by a non-crystallographic C_2 symmetry, the C_2 axis passing through the ethereal oxygen and the centroid of the four nitrogen atoms. Actually, the 12-membered tetraazamacrocycle adopts a more regular conformation than that found in the monoprotonated L1 cation, which can be described as [3333] by using the Dale's formalism.[34]

In the attempt to synthesize the Zn(II) complex with L2 in aqueous solution, we also isolated the diprotonated cation as tetrachlorozincate salt, $[H_2L2]ZnCl_4 \cdot H_2O$ (see ESI, Fig. S1).† In this compound the overall conformation of the ligand and the intramolecular hydrogen bonding pattern is very similar to that observed in $[H_2L2](ClO_4)_2$. The most significant differences can be found in the intermolecular hydrogen bonds. In fact, one NH_2^+ interacts with a chloride of the $ZnCl_4^{2-}$ anion, while the second one gives a hydrogen bonding contact with a water molecule.

Protonation of ligands in aqueous solution. The basicity properties of the cryptands L1 and L2 were preliminarily studied by means of potentiometric titrations at 298 K and the determined protonation constants are given in Table 1. L1 and L2 show similar protonation binding ability, exhibiting a high basicity in the first protonation step, and a moderate basicity in the second one. Conversely, the third protonation process takes place at very low pH values (below pH 3). In the case of L1, the first protonation constant is too high to be detected in the pH range investigated (2–11.5) and can only be estimated as higher than 12 log units. However, both receptors display a proton affinity in the first protonation step unusually high for compounds having tertiary or secondary amine functions. For instance, their first protonation constant is far higher than that found for the 12-membered tetraazamacrocycle 1,7-dimethyl-1,4,7,10-tetraazacyclododecane ($\log K_1 = 10.7$),[32c] which contains two secondary and two tertiary nitrogen atoms. Furthermore, the ^1H NMR spectrum of the ligand recorded in strongly alkaline medium (NaOH 1 M) is equal to that recorded at pH 10, where the unique species present in solution is the monoprotonated ligand $[HL1]^+$, suggesting that deprotonation of $[HL1]^+$ cannot be achieved in aqueous solutions, *e.g.*, L1 displays a proton sponge behaviour. The high proton affinity of L1 and L2 is likely to be due to their cage-like architecture and to the encapsulation of the H^+ ion within the receptor cavity. In fact, this structural feature may allow the stabilization of the $[HL]^+$ (L = L1 or L2) cation thanks to the formation of an inner-cavity hydrogen bonding network involving the oxygen atom and the amine groups of the receptors, as already observed in other cryptands based on tetraazamacrocyclic scaffolds or in reinforced tetraazamacrocycles.[36] Actually, the crystal structure of the monoprotonated cation $[HL1]^+$ shows that the H^+ ion is localized on one of the secondary nitrogen. One hydrogen atom of the NH_2^+ bond points inside the cryptand cavity, giving rise to hydrogen bonding interactions with the tertiary amine groups and the ethereal oxygen. Similar hydrogen bonding networks involving the NH_2^+ groups are also observed in the crystal structure of the protonated form of L2, $[H_2L2]^{2+}$.

Table 1 Protonation constants potentiometrically determined in NMe_4Cl 0.1 M aqueous solutions at 298 K

	Log*K*	
Reaction	L1	L2
$L + H^+ \rightleftarrows [HL]^+$	>12	11.53(2)
$[HL]^+ + H^+ \rightleftarrows [H_2L]^{2+}$	8.97(6)	9.05(3)
$[H_2L]^{2+} + H^+ \rightleftarrows [H_3L]^{3+}$	2.70(1)	2.63(4)

The crystal structures of the L1 and L2 protonated forms unequivocally show that the secondary nitrogen atoms are the preferred protonation sites of the two cryptands, in keeping with the higher basicity generally observed for secondary amine groups with respect to tertiary ones.[32c]

Protonation of the cryptands was also analysed by means of spectrophotometric and spectrofluorimetric measurements at different pH values. While the absorption spectra of L1 and L2 are basically not affected by pH, as expected considering that the dibenzofuran and diphenyl ether units in L1 and L2 are not directly involved in protonation, their fluorescence emission is strongly pH dependent. In fact, both cryptands display fluorescence emission at acidic or slightly alkaline pH values, while are weakly emissive above pH 9 (Fig. 3).

Superimposition of the fluorescence emission intensity of L1 and L2 at 316 and 292 nm, respectively, with the distribution diagrams of their protonated species (Fig. 3c and 3d), clearly shows that in both cases only the di- and triprotonated species are emissive. In the case of L1 a first marked increase of the fluorescence emission is observed with the formation of the $[H_2L1]^{2+}$ species and is subsequently followed by a further slight enhancement of fluorescence with the formation of the $[H_3L1]^{3+}$ species below pH 4. Actually, as often observed in other polyamine ligands containing fluorogenic moieties,[7–16] the polyamine scaffolds of L1 and L2 can efficiently quench the fluorescence emission of the fluorogenic units, *i.e.*, the dibenzofuran and diphenyl ether bridges, thanks to a photoinduced electron transfer (PET) process involving the lone pairs of the nitrogen atoms. Protonation of the polyamine scaffolds makes the lone pairs of the amine groups less available for the electron transfer process, leading to renewal of the fluorescence emission. The analysis of the pH-dependencies of the emission intensity indicates that binding of two H^+ ions to L1 or L2 is sufficient to produce a fluorescence enhancement. At a first glance, this behaviour could appear rather surprising considering the presence of four amine groups as potential quenchers of fluorescence. On the other hand, the crystal structure of the $[H_2L2]^{2+}$ cation shows that the NH_2^+ groups are involved in strong hydrogen bonds with the non-protonated bridgehead nitrogen

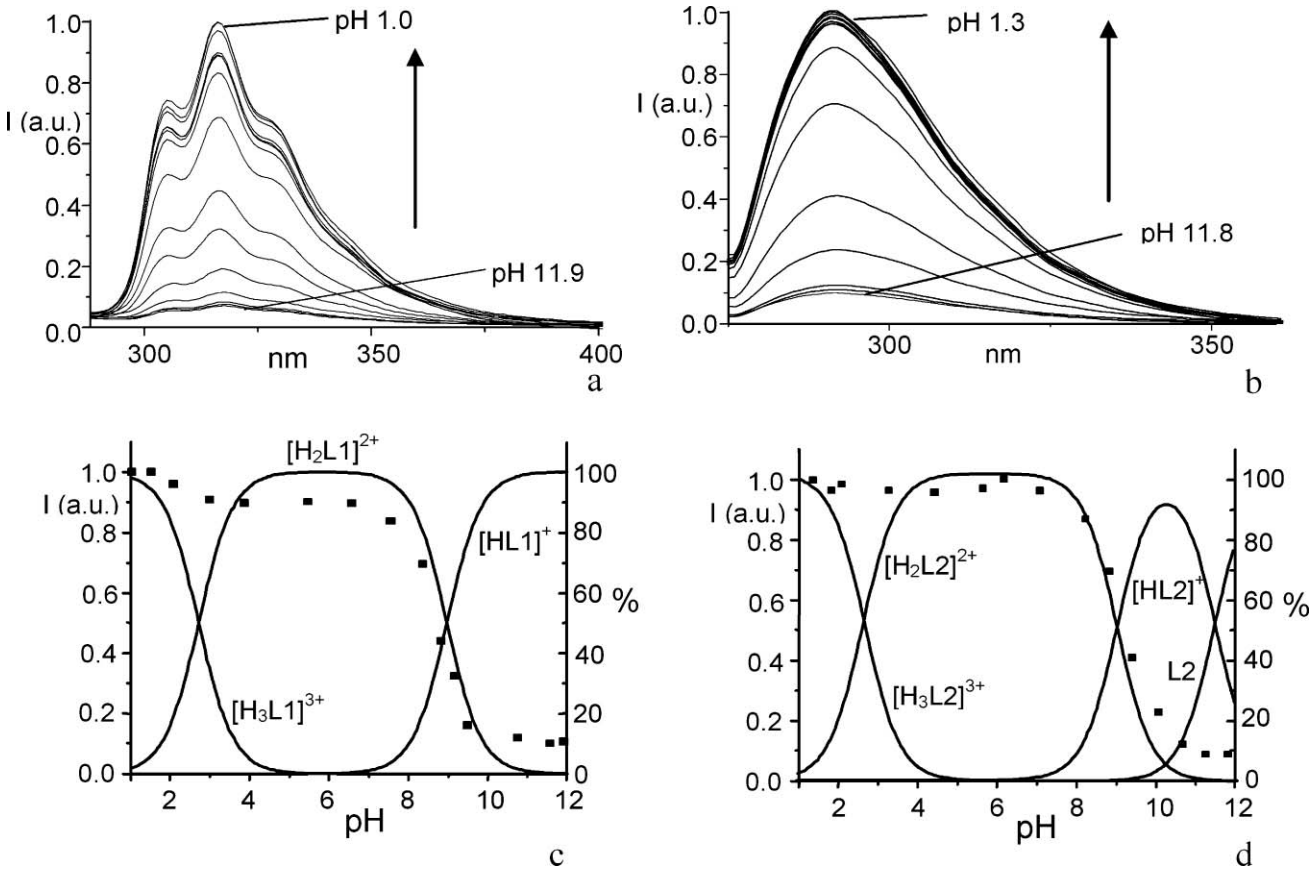

Fig. 3 Fluorescence emission spectra of L1 (a) and L2 (b) at different pH values and pH dependence of the fluorescence emission of ligand L1 at 316 nm (c) and of L2 at 293 nm (d) (■, left *y* axis) compared to the distribution diagrams of the protonated species of L1 and L2 (solid lines, right *y* axis) (0.1 M NMe_4Cl aqueous solution, 298 K) ([L1] = 4.3×10^{-6} M, λ_{exc} = 270 nm, [L2] = 5×10^{-5} M, λ_{exc} = 265 nm).

atoms, making their lone pairs less available for quenching effect.

Metal complexation

Crystal structure of [HL2ZnCl$_3$] (d). Crystals of this compound were obtained by slow evaporation at room temperature of an alkaline aqueous solution (pH 9.5) containing $ZnCl_2$ and L2 in 1 : 1 molar ratio. The ORTEP drawing of the [HL2ZnCl$_3$] complex in Fig. 4 shows that Zn(II) lies outside the cryptand cavity, coordinated to a single secondary amine group. Three chloride anions are also bound to Zn(II), affording an overall tetrahedral metal coordination geometry.

The overall conformation of L2 is very similar to that found in the crystal structure of the $[H_2L2]^{2+}$ cation. In fact, the two aromatic rings give rise to a dihedral angle of *ca.* 69°, while the conformation of the cyclen moiety can be described, following the Dale's formalism,[34] as [3333]. The apical O(1) oxygen lies 2.295(4) Å above the mean plane defined by the four nitrogen atoms. Furthermore, the protonated nitrogen N(4) and the Zn(II)-bound amine group N(2) behave as hydrogen bonding donors in a similar fashion to that observed in $[H_2L2]^{2+}$, giving rise to H-bond contacts with the bridgehead nitrogen atoms and the ethereal oxygen. All these analogies between the structures of this Zn(II) complex and of the diprotonated cation $[H_2L2]^{2+}$ seem to indicate that replacement of an H^+ ion of $[H_2L2]^{2+}$ with a Zn(II) cation in [HL2ZnCl$_3$] essentially does not alter the ligand conformation, confirming, once again, the rigidity of these small cryptands.

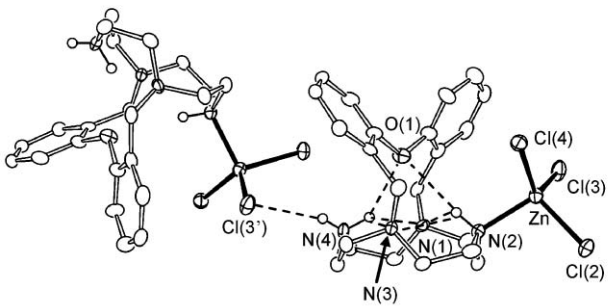

Fig. 4 ORTEP view of the [HL2ZnCl$_3$] compound (thermal ellipsoid plotted at 50% probability level). Bond distances (Å) and angles (°) for the metal coordination environment: Zn–N(2) 2.085(4), Zn–Cl(1) 2.2519(15), Zn–Cl(2) 2.2799(14), Zn–Cl(3) 2.2573(15), Cl(1)–Zn–Cl(2) 116.74(6), Cl(1)–Zn–Cl(3) 114.70(6), Cl(1)–Zn–N(2) 101.42(13), Cl(2)–Zn–Cl(3) 106.31(6), Cl(2)–Zn–N(2) 101.22(13), Cl(3)–Zn–N(2) 115.98(13). Hydrogen bonding distances (Å): N(2)–H(2C)···O(1) 2.500, N(4)–H(2)···N(1) 2.18(6), N(4)–H(2)···O(1) 2.18(6), N4–H(5)···Cl3′ 2.42(6) (symmetry relation: $1.5 - x, 2 - y, 0.5 + z$). Additional weaker hydrogen bonds, featured by somewhat low values of the N–H···N angles, which span from 100° to 120°, are also shown (N(2)–H(2C)···N(1) 2.505 Å, N(2)–H(2C)···N(3) 2.465 Å, N(4)–H(2)···N(3) 2.40(6) Å).

Finally, the protonated nitrogen also interacts *via* intermolecular hydrogen bonding a Zn(II)-bound chloride anion of a symmetry related [HL2ZnCl$_3$] complex.

Crystal structure of [CuL1](PF$_6$)$_2$·CH$_3$CN (e). The crystal structure of [CuL1](PF$_6$)$_2$·CH$_3$CN consists of [CuL1]$^{2+}$ complex cations (Fig. 5a), PF$_6^-$ anions and CH$_3$CN solvent molecules. The Cu(II) ion is located into the cavity, five-coordinated by the four nitrogen atoms and the O(1) oxygen. The resulting geometry can be best described as intermediate between a trigonal bipyramid, where the apical positions are occupied by the two tertiary nitrogen atoms and the remaining secondary nitrogen atoms and O(1) define the equatorial plane, and a square pyramid, with basal plane defined by all 4 nitrogen atoms and the apical position occupied by O(1). The copper atom lies 0.405(3) Å apart from the basal plane. Close comparison can be found in the crystal structure of complex [CuL2](ClO$_4$)$_2$ (Fig. 5b).[33] In fact, in the [CuL2]$^{2+}$ complex the Cu(II) cation is enclosed within the receptor cavity, 5-coordinated by the four nitrogen and by the oxygen of the bridge. In this case, however, the coordination geometry of the metal can be described as a square pyramid, the basal plane being defined by the 4 nitrogen donors and the oxygen atom occupying the apical position. The copper atom is 0.342 Å apart from the basal plane and the two aromatic rings give rise to a dihedral angle of 62.65°. In [CuL2]$^{2+}$ the coordination environment of the metal cation appears to be more regular than that found in the [CuL1]$^{2+}$ cation, probably due to the somewhat higher flexibility of the diphenyl ether bridge of L2. In fact, in the [CuL1]$^{2+}$ complex the planar dibenzofuran bridging group is asymmetrically bent toward one of the secondary nitrogen, preventing the oxygen atom from assuming the apical position of a square pyramidal geometrical arrangement. The different rigidity of the two cryptands can be also invoked to explain the different overall conformations of the tetraazamacrocyclic rings in [CuL1]$^{2+}$ and [CuL2]$^{2+}$. In fact, in the more flexible [CuL2]$^{2+}$ complex the cyclen unit assumes the most regular [3333] conformation, while in [CuL1]$^{2+}$ the tetraaza moiety gives rise to a more distorted and less symmetrical [2334] sequence of torsional angles.

Of note, the overall conformation of L1 and L2 in their Cu(II) complexes strongly resembles those of the corresponding protonated forms [HL1]$^+$ and [H$_2$L2]$^{2+}$, respectively. The analogies are particularly striking in the case of [CuL2](ClO$_4$)$_2$ and [H$_2$L2](ClO$_4$)$_2$. In fact, both compounds display not only almost equal conformations of the cryptand framework, but also very similar crystal packing, characterized by analogous H-bond networks involving the perchlorate anions and the secondary nitrogen atoms (see ESI, Fig. S2).† As a matter of fact, the two compounds result to be almost isomorphous. Once again, metal coordination does not significantly alter the conformations of the ligands.

Metal coordination in solution. The ability of L1 and L2 to bind transition (Cu(II), Ni(II), Co(II), Zn(II) and Cd(II)) and post-transition (Pb(II)) metal cations was analyzed by means of ^{1}H and ^{13}C NMR measurements and/or spectrophotometric and spectrofluorimetric titrations. Both ligands display a very low ability to bind metal cations in aqueous solutions. In fact, almost no change in the absorption spectra of the metal cations as well as in NMR or fluorimetric spectra of the ligands was observed by mixing aqueous solutions of ligands and metal cations in the pH range 5–9 at room temperature. No significant change was observed even after boiling the solutions for 60 h. In most cases, precipitation of metal hydroxide occurs at neutral or

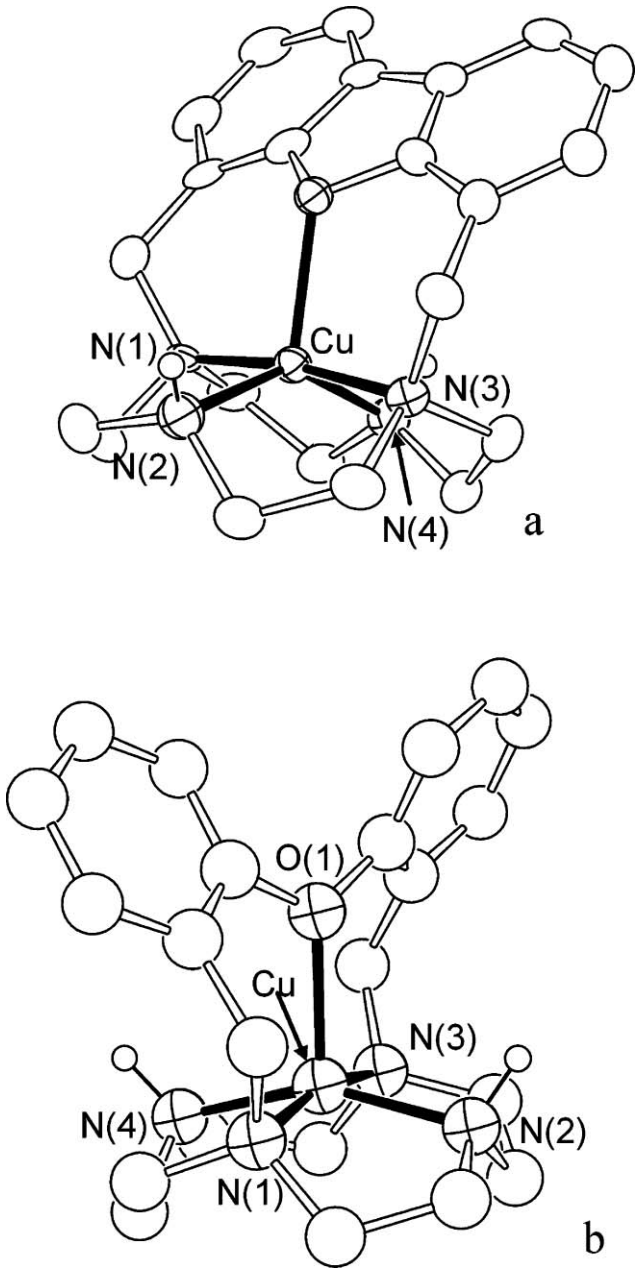

Fig. 5 ORTEP view of the [CuL1]$^{2+}$ cation (thermal ellipsoid plotted at 50% probability level) (a) and of the [CuL2]$^{2+}$ complex (b) (taken from ref. 33). Bond distances (Å) and angles (°) for the metal coordination environment in [CuL1]$^{2+}$ (Å): Cu–N(1) 2.005(6), Cu–N(2) 1.998(6), Cu–N(3) 2.008(6), Cu–N(4) 1.988(6), Cu–O(1) 2.131(5), N(2)–Cu–N(1) 90.5(2), N(1)–Cu–N(3) 171.2(2), N(1)–Cu–N(4) 88.0(2), N(2)–Cu–N(3) 86.8(2), N(2)–Cu–N(4) 141.5(3), N(3)–Cu–N(4) 88.9(2), N(1)–Cu–O(1) 93.4(2), N(2)–Cu–O(1) 112.2(2), N(3)–Cu–O(1) 95.3(2), N(4)–Cu–O(1) 106.3(2). Bond distances (Å) and angles (°) for the metal coordination environment in [CuL2]$^{2+}$ (Å): Cu–N(1) 1.9611, Cu–N(2) 2.0027, Cu–N(3) 1.9552, Cu–N(4) 2.0008, Cu–O(1) 2.1651, N(2)–Cu–N(1) 87.87, N(1)–Cu–N(3) 166.27, N(1)–Cu–N(4) 89.06, N(2)–Cu–N(3) 88.59, N(2)–Cu–N(4) 154.03, N(3)–Cu–N(4) 88.33, N(1)–Cu–O(1) 96.85, N(2)–Cu–O(1) 105.52, N(3)–Cu–O(1) 96.88, N(4)–Cu–O(1) 100.45.

slightly alkaline pH values and no dissolution is observed after prolonged boiling of the solutions. This scarce tendency to metal coordination can be related to the tight molecular architecture of cryptands L1 and L2. The very similar conformations of the cryptands in the protonated forms and in their Cu(II) complexes, observed in the solid state, account for an overall high rigidity of the ligand frameworks, which could inhibit metal complexation from a kinetic point of view. In fact, the formation of stable complexes implies metal encapsulation within the macrocyclic cavity, which can be achieved only *via* marked conformational changes of the ligand frameworks. At the same time, both ligands are featured by a small three-dimensional cavity and by a highly pre-organised disposition of the set of donor atoms, which can make the process of metal complexation unfavourable from a thermodynamic point of view. In fact, metal cations of too large dimension or featured by strict stereochemical requirements can be unable to fit the cryptand cavities or the rigid disposition of the N_4O set of donors.

However, both ligands are also characterized by a high affinity for H^+ ions. Therefore, proton binding can efficiently compete with the process of metal coordination. As a matter of fact, slow evaporation of aqueous solutions at pH 7 and 9.5 containing $ZnCl_2$ and L2 leads to crystallization of compounds $[H_2L2]ZnCl_4$ and $[HL2ZnCl_3]$, respectively. Their crystal structures may represent a nice "sketch" of the competition between proton and metal binding by L2. While in $[H_2L2]ZnCl_4$ the metal does not show any interaction with the cryptand in its diprotonated form, in $[HL2ZnCl_3]$, Zn(II) is bound, in a non-inclusive fashion, to a single secondary nitrogen of L2, while the second secondary amine group is protonated.

To shed further light on the binding ability of the two cryptands, we decided to study metal complexation in an organic solvent, such as anhydrous acetonitrile. This solvent is a less solvating agent than water and the consequent lower solvation of the metal cations can favour the process of metal complexation from both a thermodynamic and kinetic point of view. At the same time, this solvent generally ensures a good solubility of ligands, metal salts and complexes. Finally, the use of anhydrous conditions overcomes the problem of competitive process of proton binding by L1 and L2 and prevents the formation of metal hydroxo complexes or the precipitation of metal hydroxides.

Actually, addition of increasing amounts of L1 or L2 to an acetonitrile solution of $CuCl_2$ leads to a marked changes of the visible spectra of the metal, with the formation of a new band centered at 580 nm, typical of a $Cu–N_4$ chromophore, as shown in Fig. 6a for L2 (the visible spectra recorded on solution containing Cu^{2+} and L1 are reported in the ESI, Fig. S3).† As shown in Fig. 6b, the absorbance at 580 nm increases linearly up to a 1 : 1 Cu(II) to L2 molar ratio, to achieve a constant value in the presence of a slight excess of Cu(II). These data account for the formation of a complex, containing Cu(II) encapsulated within the cavity of the cryptands. Actually, slow evaporation of non-aqueous solutions containing Cu(II) and L1 or L2 leads to crystallization of the $[CuL1]^{2+}$ and $[CuL2]^{2+}$ [33] complexes, both containing the metal encapsulated within the cryptand cavities.

Conversely, addition of L1 or L2 to solutions of $NiCl_2$ or $CoCl_2$ show only slight changes in the absorption spectra of the metals (a 5–10 nm blue-shift of the band in the visible region of the spectrum). No change in the spectra was observed even after

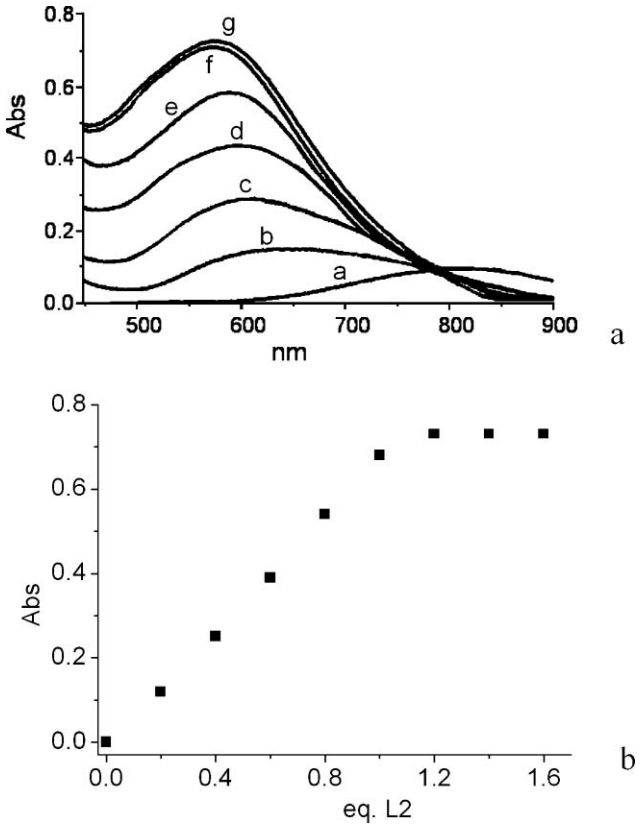

Fig. 6 (a) Visible spectra of Cu(II) in acetonitrile in the presence of increasing amounts of L2 (equiv. of L2: a, 0; b, 0.2; c, 0.4; d, 0.6; e, 0.8; f, 1.0; g 1.2 or more); (b) absorbance at 580 nm in the presence of increasing amounts of L2. The samples were heated at 45 °C for 5 min after each addition of Cu(II) to the solution of L2, in order to ensure complete formation of the complexes. The spectra were then recorded at room temperature.

prolonged heating of the solution (60 h) at 70° C. These results indicate that these metal cations do not interact or interact very weakly with the ligands and rule out metal complexation in an inclusive fashion. Most likely, the stereochemical requirements of Ni(II) or Co(II), stricter than those of Zn(II) or Cu(II), prevent their coordination by the N_4O donor set, rigidly organized within the cryptand cavities.

Zn(II), Cd(II) and Pb(II) complexation was first analyzed by recording ^1H and ^{13}C NMR spectra in acetonitrile. The ^{13}C NMR spectrum of L1 shows three signals in the aliphatic region of the spectrum, at 48.6 ppm (attributed to the carbon atoms belonging to the ethylenic chains and adjacent to the secondary nitrogen atoms), 52.5 ppm (the carbon atoms of the ethylenic chains adjacent to the tertiary nitrogen atoms) and 58.3 ppm (the benzylic carbon) and six signals for the dibenzofuran unit, assigned to the carbon atoms of a single benzene unit. These spectral features may account for a C_{2v} time-averaged symmetry, generated by a C_2 axis perpendicular to the plane of the cyclen unit and a symmetry plane passing through the two secondary nitrogen atoms and containing the C_2 axis. The L2 spectrum is composed by five signals in the aliphatic region, four of which assigned to the carbon atoms of two non-equivalent ethylenic chains and one to the benzylic methylene carbons and six resonances for the aromatic moiety, attributed to a single benzene ring. These spectral features accounts for a C_2

time-averaged symmetry of the cryptand, due to the presence of a C_2 axis perpendicular to the plane of the four nitrogen atoms and passing through the oxygen atom of the bridge. The ^{13}C NMR spectra of L1 and L2 are shown in Fig. S4 and S5 (ESI),† while the aliphatic portion of the L2 spectrum is shown in Fig. 7. The ^{1}H spectra are less informative, due to partial overlapping of the signals (ESI, Fig. S4 and S5).† However, in the case of L2 some signals are clearly recognizable and substantially confirm the proposed C_2 symmetry of this molecule (Fig. 7).

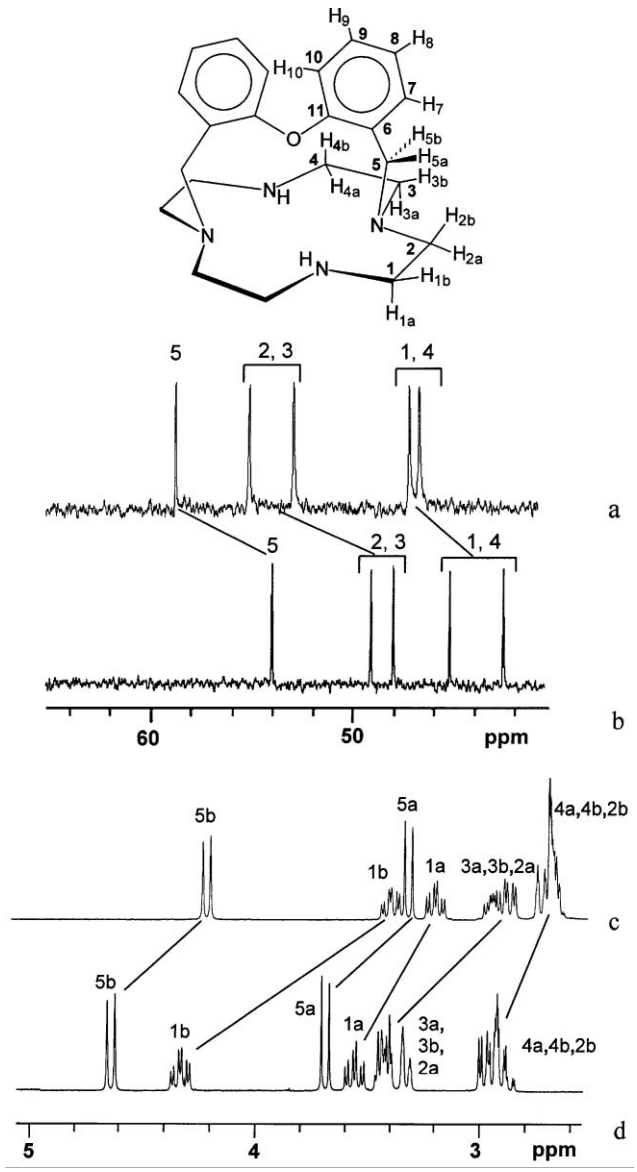

Fig. 7 Aliphatic region of the $^{13}C\{^{1}H\}$ and ^{1}H NMR spectra of L2 in CD_3CN in the absence (a, c) and in the presence of 1 equiv. of Zn(II) (b, d). The samples were heated at 45 °C for 5 min after the addition of Zn(II) to the solution of L2, in order to ensure complete formation of the complex. The spectra were then recorded at room temperature.

Changes of these spectral features can be used to monitor metal complexation. As a matter of fact, both the ^{1}H and ^{13}C NMR spectra of L1 and L2 are almost not affected by the presence of 1 equiv. of Cd(II) or Pb(II), even after prolonged heating (60 h) of the solutions at 70° C. Conversely, addition of Zn(II) (1 equiv.) does not change the symmetry of the cryptands, but leads to a marked upfield shift of the ^{13}C signals in the aliphatic region of the spectrum and to an overall downfield shift of the ^{1}H resonances of the aliphatic hydrogens (see Fig. 7 for L2). Minor shift are also observed for the ^{1}H and ^{13}C NMR aromatic signals (ESI, Fig. S4 and S5).† These results suggest the formation of stable Zn(II) complexes in solutions. Slow evaporation of these solution in the presence of $NaClO_4$ lead to the isolation of solid compounds with $[ZnL1](ClO_4)_2$ and $[ZnL2](ClO_4)_2{\cdot}CH_3CN$ stoichiometries. Solutions of these compounds in deuterated acetonitrile displayed ^{1}H and ^{13}C NMR spectra equal to that obtained by addition of 1 equiv. of Zn(II) to solutions of the ligands. Although no crystal suitable for X-ray analysis was obtained, it can be reasonably proposed that the metal is enclosed within the receptor cavity. Conversely, Pb(II) and Cd(II) are probably too large to be coordinated inside the small cavities of these receptors.

Metal complexation was also analyzed by means of spectrofluorimetric titrations. Cryptands L1 and L2 are weakly emissive in acetonitrile, probably due to the electron transfer process involving the amine lone pairs which quench the fluorescence emission. Addition of Zn(II) gives rise to a marked increase of the fluorescence emission of both cryptands, as shown in Fig. 8. Once again, the fluorescence emission intensity increases almost linearly up to a 1 : 1 metal to ligand molar ratio is reached and achieves a constant values for molar ratios greater than 1. This indicates the formation of stable complexes between Zn(II) and the cryptands. At the same time, the marked fluorescence increase is likely to be due to the inhibition of the PET effect from the amine groups of L1 or L2 to the excited fluorophore, suggesting that the lone pairs of the amine donors are involved in metal complexation, in keeping with the hypothesis that Zn(II) is bound by the two cryptands in an inclusive fashion.

Addition of Ni(II) or Co(II) does not significantly affect the weak fluorescence emission of the ligands, while addition of Cu(II) leads to further decrease of the emission intensity (Fig. 9), as expected for the coordination of a paramagnetic metal ion. Similarly to Ni(II) and Co(II), the presence of Cd(II) or Pb(II) does not alter the emission of L1 and L2. These results are in agreement with the suggested scarce interaction of Co(II), Ni(II), Cd(II) and Pb(II), proposed on the basis of the NMR or UV-vis measurements.

Therefore, L1 and L2 are able not only to selectively bind Zn(II) and Cu(II) over various transition metal and post-transition cations, but also to selectively signal Zn(II) complexation thanks to a fluorescence emission enhancement.

Conclusion

L1 and L2 display a rigid molecular architecture, characterized by a small inner cavity and a pre-organized disposition of the set of donor atoms. These structural features strongly affect both protonation and metal binding characteristics of the two cryptands. In fact, the ammonium groups formed upon ligand protonation give rise to an inner-cavity hydrogen bonding network, which stabilized the protonated forms of the cryptands. Ligand rigidity, small cavity dimension and/or high basicity make unfavoured metal complexation in water, preventing the possible use of these cryptands as selective metal ion binders, at least in aqueous solutions. On the other hand, the rigid molecular architecture leads to a marked selectivity in metal ion binding in non-aqueous

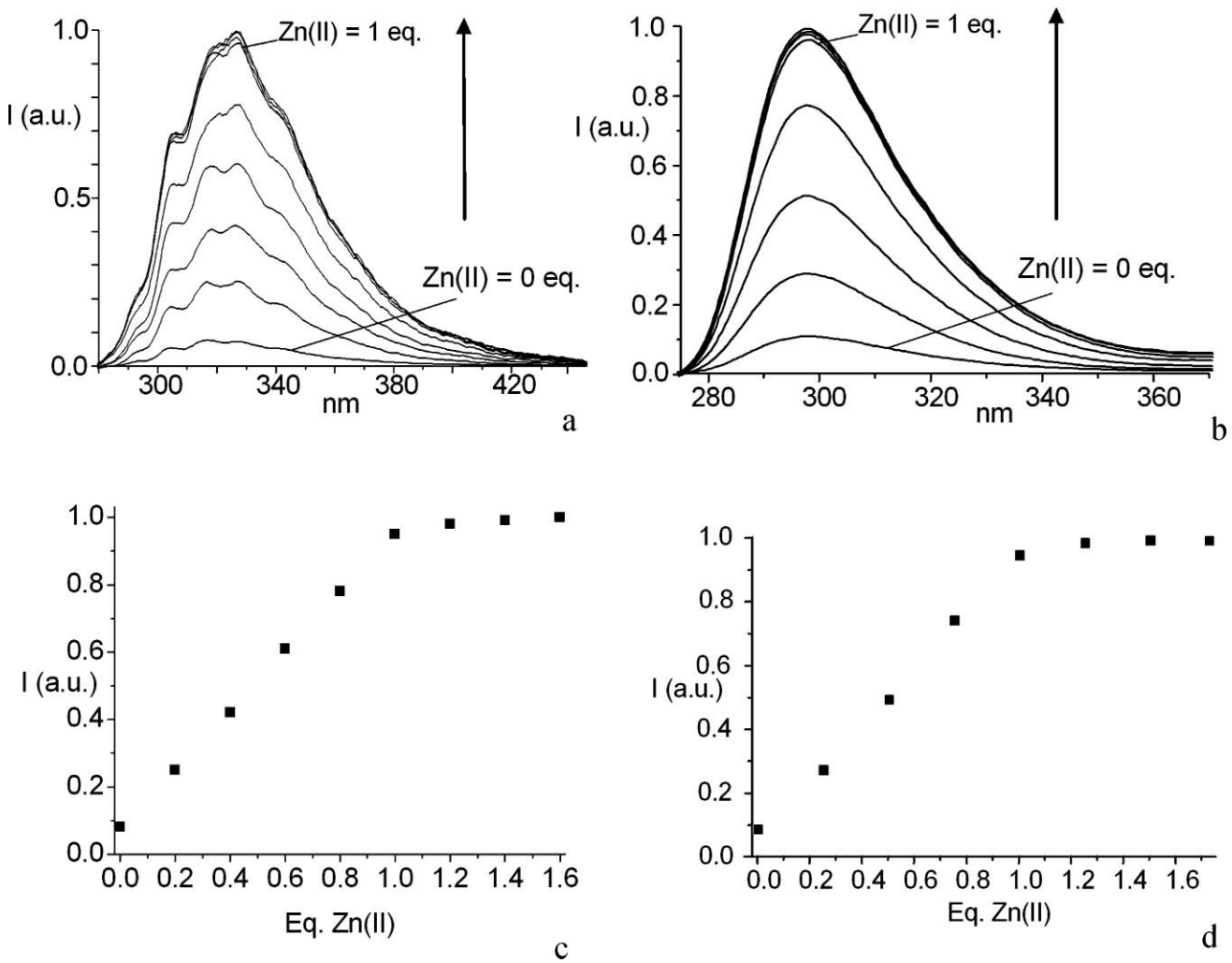

Fig. 8 Emission spectra of L1 (a) and L2 (b) and fluorescence emission intensity of L1 at 330 nm (c) and of L2 at 293 nm (d) in acetonitrile in the presence on increasing amounts of Zn(II) ([L1] = 5.0×10^{-6} M, [L2] = 5.0×10^{-5} M). The spectra were recorded at 298 K after successive addition of 0.2 (in the case of L1) or 0.25 equiv. of Zn(II) (in the case of L2). The samples were heated at 45 °C for 5 min after each addition of Zn(II) to the solution of L1 or L2, in order to ensure complete formation of the complexes. The spectra were then recorded at room temperature.

solvent (acetonitrile), where both cryptands selectively coordinate Zn(II) and Cu(II) over Ni(II), Co(II), Cd(II) and Pb(II). Of note, Zn(II) encapsulation within the receptor cavity is accompanied by a remarkable increase of the fluorescence emission intensity. These results can be useful to develop new selective fluorescent chemosensors based on cryptand-like architectures. In particular, the use of more flexible propylenic chains linking the nitrogen donors and/or the replacement of the secondary amine groups with less basic tertiary amine groups can allow overcoming the major limits of these receptors, and we are working in this direction.

Experimental

General procedures

In all measurements L1 and L2 were used as such or as triperchlorate salts, obtained in almost quantitative yields by addition of concentrated $HClO_4$ to ethanol solutions of the free amines. Caution: perchlorate salts of metal complexes with organic ligands are potentially explosive and should be handled with care.

Synthesis of the compounds

Synthesis of L1. A solution of dibenzofuran-4,6-dicarbaldehyde (1.22 g, 5.46 mmol) in 1,2-dichloroethane (20 mL) was added dropwise to a stirred solution of 1,4,7,10-tetraazacyclododecane (cyclen) (0.94 g, 5.46 mmol) and fresh sodium triacetoxyborohydride (3.24 g, 15.28 mmol) in 1,2 dichloroethane (100 mL). The solution was stirred at room temperature under an atmosphere of nitrogen for 48 h. The reaction mixture was quenched by addition of a 1 M NaOH aqueous solution (150 mL), and the product extracted with chloroform (3 × 100 mL). The organic layer was dried over $MgSO_4$ and evaporated under reduce pressure. The crude product was washed with cyclohexane to give the compound L1 as a yellow powder (1.49 g, 75%). δ_H (500 MHz, $CDCl_3$): 2.50 (bs, 2 H), 2.53 (m, 8 H), 2.64 (m, 8 H), 4.00 (s, 4 H), 7.18 (m, 4 H), 7.79 (m, 2 H); δ_C (125 MHz, $CDCl_3$): 47.9, 53.0, 58.6, 120.9, 123.1,

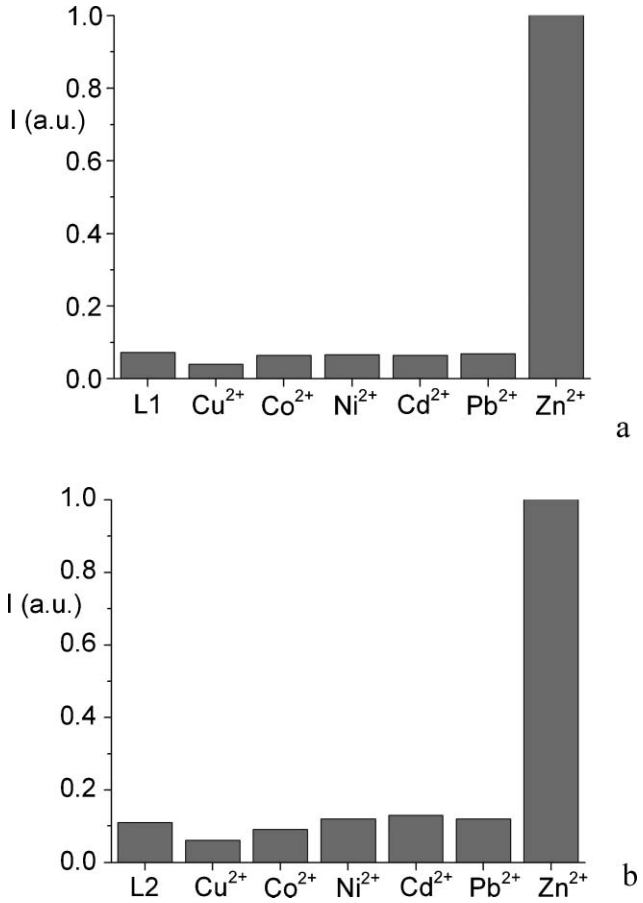

Fig. 9 Comparison between the fluorescence emission of L1 (a) and L2 (b) alone in acetonitrile and in the presence of 1 equiv. of various metal cations ([L1] = 5.0×10^{-6} M, [L2] = 5.0×10^{-5} M).

124.4, 125.5, 128.7, 154.8; Anal. calcd for $C_{22}H_{28}N_4O$ (MW = 364.49) C 72.50, H 7.74, N 15.37. Anal. found: C 72.3, H 7.8, N 15.3; *m/z* (MALDI-TOF) 364.9.

Synthesis of L2. L2 was obtained from cyclen (0.78 g, 4.53 mmol) and bis(2-formylphenyl)ether (1.02 g, 4.53 mmol) in the presence of sodium triacetoxyborohydride (2.69 g, 12.68 mmol) by using the same procedure reported for L1. The compound was isolated as a white powder (1.29 g, 78%). δ_H (500 MHz, $CDCl_3$): 2.05 (bs, 2 H), 2.45–2.82 (m, 16 H), 3.33 (d, J = 12.5 Hz, 2 H), 4.13 (d, J = 12.5 Hz, 2 H), 6.65 (m, 2 H), 6.96 (m, 2 H), 7.15 (m, 4 H); δ_C (125 MHz, $CDCl_3$): 48.1, 48.4, 53.5, 55.9, 59.2, 119.3, 123.7, 130.0, 130.9, 132.5, 157.3; Anal. calcd for $C_{22}H_{28}N_4O$ (MW = 366.51) C 72.08, H 8.26, N 15.29. Anal. found: C 72.0, H 8.3, N 15.2; *m/z* (MALDI-TOF) 367.1.

{[HL1]L1}$ClO_4 \cdot 3.5H_2O$. This compound was obtained in the attempt to obtain L1 as free amine starting from its triperchlorate salt (L1·3$HClO_4$). L1·3$HClO_4$ (50 mg, 0.073 mM) was dissolved in NaOH 5 M. The resulting solution was extracted four times with $CHCl_3$. The organic layer was then separated, dried on Na_2SO_4 and filtrated. Slow evaporation of the resulting solutions afforded crystals of {[HL1]L1}$ClO_4 \cdot 3.5H_2O$. Yield: 36.3 mg (64.3%). Anal. calcd for $C_{44}H_{64}ClN_8O_{9.5}$ (MW = 892.48) C 59.21, H 7.23, N 12.56. Anal. found: C 59.4, H 7.3, N 12.3.

[ZnL1]$(ClO_4)_2$. A solution of $Zn(ClO_4)_2 \cdot 6H_2O$ (10.0 mg, 0.027 mM) in 5 mL CH_3CN was slowly added to a boiling solution of L1 (10 mg, 0.027 mM) in CH_3CN (15 mL). The resulting solution was cooled at room temperature. Slow evaporation of the solution afforded the complex as a colourless powder. Yield: 14.5 mg (85.6%). Anal. calcd for $C_{22}H_{28}Cl_2N_4O_9Zn$ (MW = 628.8) C 42.09, H 4.49, N 8.91. Anal. found: C 42.0, H 4.5, N 8.8.

[H_2L2]$(ClO_4)_2$. This compound was obtained from slow evaporation of an aqueous solution (10 mL) at pH 6 containing L2 (10 mg, 0.027 mM) and an excess of $NaClO_4$ (50 mg). Yield: 11.2 mg (73.2%). Anal. calcd for $C_{22}H_{32}Cl_2N_4O_9$ (MW = 567.42) C 46.63, H 5.70, N 12.35. Anal. found: C 46.4, H 5.8, N 12.2.

[H_2L2]$(ZnCl_4) \cdot H_2O$. This compound was obtained from slow evaporation of an aqueous solution (10 mL) at pH 7 containing L2 (10 mg, 0.027 mM) and $ZnCl_2$ (3.7 mg, 0.027 mM). Yield: 11.8 mg (73.6%). Anal. calcd for $C_{22}H_{34}Cl_4N_4O_2Zn$ (MW = 593.70) C 44.51, H 5.77, N 9.44. Anal. found: C 44.5, H 5.8, N 9.3.

[HL2$ZnCl_3$]. This compound was obtained form an aqueous solution at pH 9.5 by using the same procedure reported for [H_2L2]$(ZnCl_4) \cdot H_2O$. Yield: 12.7 mg (87.4%). Anal. calcd for $C_{22}H_{31}Cl_3N_4OZn$ (MW = 539.25) C 49.00, H 5.79, N 10.39. Anal. found: C 48.8, H 5.9, N 10.3.

[ZnL2]$(ClO_4)_2 \cdot CH_3CN$. This complex was obtained from $Zn(ClO_4)_2 \cdot 6H_2O$ and L2 by using the same procedure reported for [ZnL1]$(ClO_4)_2$. Yield: 15.4 mg (84.9%). Anal. calcd for $C_{24}H_{33}Cl_2N_5O_9Zn$ (MW = 671.8) C 42.91, H 4.95, N 10.42. Anal. Found: C 42.8, H 4.9, N 10.4.

[CuL1]$(PF_6)_2 \cdot CH_3CN$. A solution of $CuCl_2$ (3.6 mg, 0.027 mM) in CH_3CN (5 mL) was slowly added to a boiling solution of L1 (10 mg, 0.027 mM) in CH_3CN (20 mL). The resulting solution then was cooled at room temperature and an excess of KPF_6 (20 mg) was added. Slow evaporation of the solution afforded crystal of the complex. Yield: 16.4 mg (80.2%). Anal. calcd for $C_{24}H_{35}F_{12}P_2N_5OCu$ (MW = 759.0) C 37.98, H 4.12, N 9.23. Anal. Found: C 37.9, H 4.2, N 9.1.

Single-crystal X-ray diffraction analyses

Data for the X-ray structural analyses of {[HL1]L1}$ClO_4 \cdot 3.5H_2O$ (a), [H_2L2]$(ClO_4)_2$ (b), [H_2L2]$ZnCl_4 \cdot H_2O$ (c), [HL2$ZnCl_3$] (d) and [CuL1]$(PF_6)_2 \cdot CH_3CN$ (e) were collected using Oxford Diffraction Xcalibur3 diffractometers equipped with CCD area detector and graphite monochromated Cu-Kα radiation in the case of (a) and (d) and Mo-Kα in the case of (b), (c) and (e). A summary of crystal data and structure refinement is reported in Table 2. Data collections were performed using a ω scan with the CrysAlis CCD program.[37] Crystals of almost all compounds were of poor quality, so limiting the highest resolution to 0.9 Å. Data reduction was carried out with the CrysAlis Red program,[38] and an empirical absorption correction was applied using spherical harmonics, implemented with the SCALE3 ABSPACK scaling algorithm.[38] Structures were solved by direct methods (SIR2004)[39] and refined against F^2 by using SHELXL-97.[40] All non-hydrogen atoms were anisotropically refined, except for some disordered water oxygen in (a), which were isotropically refined. All hydrogen atoms were introduced in calculated positions and refined in agreement with the linked atoms. Atoms H(1), H(2), H(3), H(4)

Table 2 Crystal data and structure refinement for {[HL1]L1}$ClO_4 \cdot 3.5H_2O$ (a), $[H_2L2](ClO_4)_2$ (b), $[H_2L2]ZnCl_4 \cdot H_2O$ (c), $[HL2ZnCl_3]$ (d), $[CuL1](PF_6)_2 \cdot CH_3CN$ (e)

	(a)	(b)	(c)	(d)	(e)
Empirical formula	$C_{44}H_{64}ClN_8O_{9.5}$	$C_{22}H_{32}Cl_2N_4O_9$	$C_{22}H_{34}Cl_4N_4O_2Zn$	$C_{22}H_{31}Cl_3N_4OZn$	$C_{24}H_{31}CuF_{12}N_5OP_2$
Formula weight	892.48	567.42	593.70	539.23	759.02
T/K	150	298	298	298	150
Space group	$P2_1/c$	$P2_1/n$	$P2_1/c$	$P2_12_12_1$	$P2_1/n$
a/Å	10.5000(2)	12.2267(9)	9.9245(3)	8.7838(2)	11.3780(9)
b/Å	23.3006(7)	13.5562(9)	15.6324(5)	14.7915(3)	19.190(2)
c/Å	19.3576(5)	15.544(1)	17.8004(6)	18.3776(3)	13.479(1)
α/°	90	90	90	90	90
β/°	99.935(3)	95.713(7)	100.571(4)	90	92.338(7)
γ/°	90	90	90	90	90
V/Å^3	4664.9(2)	2563.6(3)	2714.8(2)	2387.72(8)	2940.5(4)
Z	4	4	4	4	4
Independent reflections/R_{int}	6624/0.0892	3442/0.0773	3703/0.0375	4358/0.0691	5147/0.0483
μ/mm^{-1}	1.244 (Cu-Kα)	0.312 (Mo-Kα)	1.325 (Mo-Kα)	4.691 (Cu-Kα)	0.958 (Mo-Kα)
Flack parameter	—	—	—	0.05(3)	—
R indices $[I > 2\sigma(I)]^a$	$R_1 = = 0.0827$ $wR_2 = 0.2102$	$R_1 = 0.0815$ $wR_2 = 0.1941$	$R_1 = 0.0855$ $wR_2 = 0.2322$	$R_1 = 0.0441$ $wR_2 = 0.0852$	$R_1 = 0.0807$ $wR_2 = 0.2220$
R indices (all data)^a	$R_1 = 0.1841$ $wR_2 = 0.2568$	$R_1 = 0.1585$ $wR_2 = 0.2329$	$R_1 = 0.1200$ $wR_2 = 0.2322$	$R_1 = 0.0725$ $wR_2 = 0.1076$	$R_1 = 0.1136$ $wR_2 = 0.2401$

^{a} $R_1 = \Sigma \| F_o | - | F_c \| / \Sigma | F_o |$; $wR_2 = [\Sigma w(F_o^2 - F_c^2)^2 / \Sigma w F_o^4]^{\frac{1}{2}}$

and H(5) in (a) and H(2) and H(5) in (d), linked to nitrogen atoms, were localized in the Fourier difference maps, introduced in the calculations and isotropically refined. In complex (e) a residual peak (Q1) was found in the electron density map at the end of refinement at short distance from the copper atom (Q1 $\cdots$ N(1) 0.94 Å, Q1 $\cdots$ Cu 1.07 Å), due to local truncation errors of the series.

Potentiometric measurements

Equilibrium constants for protonation of L1 and L2 were determined by pH-metric measurements at 298.1 ± 0.1 K in 0.1 M NMe_4Cl, by using equipment and procedures,[15] which have been already described. Three titrations (about 100 data points for each one) were performed in the pH range 2–12. The computer program HYPERQUAD[41] was used to calculate equilibrium constants from emf values.

Spectrophotometric and spectrofluorimetric measurements

Absorption spectra were recorded on a Perkin-Elmer Lambda 25 spectrophotometer. Fluorescence emission spectra were collected on a Perkin Elmer LS55 spectrofluorimeter. In the experiments in aqueous solutions at different pH values HCl and NaOH were used to adjust the pH values which were measured on a Metrohm 713 pH meter. In the measurements in CH_3CN, the samples were heated at 45 °C for 5 min after each addition of Cu(II) or Zn(II) to the solution of L1 or L2, in order to ensure complete formation of the complexes. The spectra were then collected at room temperature. In the case of Co(II), Ni(II) Cd(II) or Pb(II), the spectra were collected at room temperature after heating the solutions at 70 °C for prolonged times (up to 60 h). The spectra are equal to those recorded immediately after the addition at room temperature of the metal salt to solutions of the ligands.

NMR spectroscopy

^1H and ^{13}C spectra, ^1H–^1H homonuclear and ^1H–^{13}C heteronuclear correlation experiments were carried out in CD_3CN solutions on a Bruker Avance 400 MHz spectrometer, or in $CDCl_3$ solutions on a Bruker Avance 500 MHz spectrometer. The spectra recorded on solutions containing L1 or L2 in CH_3CN in the presence of 1 eq. of the different metal cations were collected at room temperature after heating the solutions for 5 min at 45 °C. Prolonged heating of solutions (up to 60 h at 70 °C) does not change the spectral features.

Acknowledgements

Financial support by MIUR within the PRIN 2007 program is gratefully acknowledged

References

1 (*a*) L. F. Lindoy, *The Chemistry of Macrocyclic Ligand Complexes*, Cambridge University Press, Cambridge, UK, 1989; (*b*) L. F. Lindoy, *Pure Appl. Chem.*, 1997, **69**, 2179–2186.
2 J. S. Bradshaw, *Aza-crown Macrocycles*, Wiley, New York, 1993.
3 (*a*) K. B. Mertes, J. M. Lehn, in *Comprehensive Coordination Chemistry*, ed. G. Wilkinson, Pergamon, Oxford, 1987, pp. 915–1009; (*b*) J. M. Lehn, *Supramolecular Chemistry* VCH, New York, 1995.
4 P. Guerriero, S. Tamburini and P. A. Vigato, *Coord. Chem. Rev.*, 1995, **139**, 17–243.
5 J. Nelson, V. McKee, G. Morgan, in *Progr. Inorg. Chem.*, ed. K. D. Karlin, Wiley, New York, 1998, 47, pp. 167–213.
6 L. Prodi, M. Montalti, N. Zaccheroni, L. S. Dolci, in *Topics in Fluorescence Spectroscopy*, *Vol. 9*, ed. C. D. Geddes and J. R. Lakowicz, Springer, New York, 2005, pp. 1–57.
7 (*a*) L. Fabbrizzi, M. Licchelli, G. Rabaioli and A. Taglietti, *Coord. Chem. Rev.*, 2000, **205**, 85–108; (*b*) V. Amendola, M. Bonizzoni, D. Esteban-Gomez, L. Fabbrizzi, M. Licchelli, F. Sancenon and A. Taglietti, *Coord. Chem. Rev.*, 2006, **250**, 1451–1470; (*c*) V. Amendola, L. Fabbrizzi, F. Foti, M. Licchelli, C. Mangano, P. Pallavicini, A. Poggi, D. Sacchi and A. Taglietti, *Coord. Chem. Rev.*, 2006, **250**, 273–299.
8 A. P. de Silva, D. B. Fox, A. J. M. Huxley and T. S. Moody, *Coord. Chem. Rev.*, 2000, **205**, 41–57.

9 (*a*) F. Pina, M. A. Bernardo and E. Garcia-España, *Eur. J. Inorg. Chem.*, 2000, 2143–2157; (*b*) A. J. Parola, J. C. Lima, C. Lodeiro, F. Pina, in *Fluorescence of Supermolecules, Polymers, and Nanosystems, Springer Series on Fluorescence*, vol. 4, ed. M. N. Berberan-Santos, Springer, Berlin, 2008, pp. 117–149.

10 (*a*) F. Denat, Y. A. Diaz-Fernandez, L. Pasotti, N. Sok and P. Pallavicini, *Chem.–Eur. J.*, 2010, **16**, 1289–1295; (*b*) F. Denat, Y. A. Diaz-Fernandez, P. Pallavicini, L. Pasotti, Y. Rousselin and N. Sok, *Dalton Trans.*, 2009, 6751–6758; (*c*) S. Goubert-Renaudin, M. Etienne, S. Brandes, M. Meyer, F. Denat, B. Lebeau and A. Walcarius, *Langmuir*, 2009, **25**, 9804–9813; (*d*) E. Ranyuk, D. Morkos, C. Douaihy, A. Bessmertnykh, F. Denat, A. Averin, I. Beletskaya and R. Guilard, *Org. Lett.*, 2009, **11**, 987–990.

11 P. Pallavicini, Y. A. Diaz-Fernandez and L. Pasotti, *Coord. Chem. Rev.*, 2009, **253**, 2226–2240.

12 (*a*) P. Teolato, E. Rampazzo, M. Arduini, F. Mancin, P. Tecilla and U. Tonellato, *Chem.–Eur. J.*, 2007, **13**, 2238–2245; (*b*) F. Mancin, E. Rampazzo, P. Tecilla and U. Tonellato, *Chem.–Eur. J.*, 2006, **12**, 1844–1854.

13 (*a*) M. C. Aragoni, M. Arca, A. Bencini, A. J. Blake, C. Caltagirone, G. De Filippo, F. A. Devillanova, A. Garau, T. Gelbrich, M. B. Hursthouse, F. Isaia, V. Lippolis, M. Mameli, P. Mariani, B. Valtancoli and C. Wilson, *Inorg. Chem.*, 2007, **46**, 4548–4559; (*b*) A. Danesi, F. A. Devillanova, A. Garau, T. Gelbrich, F. Isaia, V. Lippolis, M. B. Hursthouse, B. Valtancoli and C. Wilson, *Inorg. Chem.*, 2007, **46**, 8088–8097; (*c*) M. C. Aragoni, M. Arca, A. Bencini, A. J. Blake, C. Caltagirone, G. De Filippo, F. A. Devillanova, A. Garau, T. Gelbrich, M. B. Hursthouse, F. Isaia, V. Lippolis, M. Mameli, P. Mariani, B. Valtancoli and C. Wilson, *Inorg. Chem.*, 2007, **46**, 4548–4559.

14 (*a*) G. Ambrosi, M. Formica, V. Fusi, L. Giorgi, E. Macedi, M. Micheloni and R. Pontellini, *Inorg. Chim. Acta*, 2009, **362**, 2667–2677; (*b*) G. Ambrosi, C. Battelli, M. Formica, V. Fusi, L. Giorgi, E. Macedi, M. Micheloni, R. Pontellini and L. Prodi, *New J. Chem.*, 2009, **33**, 171–180.

15 (*a*) C. Bazzicalupi, A. Bencini, A. Bianchi, L. Borsari, A. Danesi, C. Giorgi, C. Lodeiro, P. Mariani, F. Pina, S. Santarelli, A. Tamayo and B. Valtancoli, *Dalton Trans.*, 2006, 4000–4010; (*b*) C. Bazzicalupi, A. Bencini, E. Berni, A. Bianchi, A. Danesi, C. Giorgi, B. Valtancoli, C. Lodeiro, J. C. Lima, F. Pina and A. M. Bernardo, *Inorg. Chem.*, 2004, **43**, 5134–5146.

16 (*a*) J. Pina, J. Seixas de Melo, F. Pina, C. Lodeiro, J. C. Lima, A. J. Parola, C. Soriano, M. P. Clares, M. T. Albelda, R. Aucejo and E. Garcia-España, *Inorg. Chem.*, 2005, **44**, 7449–7458; (*b*) J. Alarcon, M. T. Albelda, R. Belda, M. P. Clares, E. Delgado-Pinar, J. C. Frias, E. Garcia-España, J. Gonzalez and C. Soriano, *Dalton Trans.*, 2008, 6530–6538.

17 (*a*) R. M. F. Batista, E. Oliveira, S. P. G. Costa, C. Lodeiro and M. Raposo, *Tetrahedron Lett.*, 2008, **49**, 6575–6578; (*b*) A. Tamayo, B. Pedras, C. Lodeiro, L. Escriche, J. Casabo, J. L. Capelo, B. Covelo, R. Kivekas and R. Sillanpaa, *Inorg. Chem.*, 2007, **46**, 7818–7826.

18 (*a*) M. Boiocchi, L. Fabbrizzi, M. Licchelli, D. Sacchi, M. Vazquez and C. Zampa, *Chem. Commun.*, 2003, 1812–1813; (*b*) L. Fabbrizzi, F. Foti, M. Licchelli and A. Poggi, *Inorg. Chem.*, 2002, **41**, 4612–4614.

19 (*a*) J. V. Ros-Lis, R. Martinez-Manez, F. Sancenon, J. Soto, M. Spieles and K. Rurack, *Chem.–Eur. J.*, 2008, **14**, 10101–10114; (*b*) J. V. Ros-Lis, R. Martinez-Manez, K. Rurack, F. Sancenon, J. Soto and M. Spieles, *Inorg. Chem.*, 2004, **43**, 5183–5185.

20 S. J. Lippard, *Chem. Rev.*, 2008, **108**, 3443–3480.

21 G. Farruggia, S. Iotti, L. Prodi, M. Montalti, N. Zaccheroni, P. B. Savage, V. Trapani, P. Sale and F. Wolf, *J. Am. Chem. Soc.*, 2006, **128**, 344–350.

22 C. Bazzicalupi, A. Bencini, S. Biagini, A. Bianchi, E. Faggi, C. Giorgi, M. Marchetta, F. Totti and B. Valtancoli, *Chem.–Eur. J.*, 2009, **15**, 8049–8063.

23 C. Bazzicalupi, A. Bencini, A. Bianchi, A. Danesi, E. Faggi, C. Giorgi, S. Santarelli and B. Valtancoli, *Coord. Chem. Rev.*, 2008, **252**, 1052–1068.

24 C. Bazzicalupi, A. Bencini, L. Bussotti, E. Berni, S. Biagini, E. Faggi, P. Foggi, C. Giorgi, A. Lapini, A. Marcelli and B. Valtancoli, *Chem. Commun.*, 2007, 1230–1232.

25 (*a*) F. Barigelletti, L. De Cola, V. Balzani, P. Belser, A. Von Zelewsky, F. Vögtle, F. Ebmeyer and S. Grammenudi, *J. Am. Chem. Soc.*, 1989, **111**, 4662–4668; (*b*) V. Balzani, R. Ballardini, F. Bolletta, M. T. Gandolfi, A. Juri, M. Maestri, M. F. Manfrin, L. Moggi and N. Sabbatini, *Coord. Chem. Rev.*, 1993, **125**, 75–88 and references therein; (*c*) N. Sabbatini, M. Guardigli and J.-M. Lehn, *Coord. Chem. Rev.*, 1993, **123**, 201–228; (*d*) V. Balzani, A. Credi and M. Venturi, *Coord. Chem. Rev.*, 1998, **171**, 3–16, and references therein.

26 (*a*) G. Ambrosi, P. Dapporto, M. Formica, V. Fusi, L. Giorgi, A. Guerri, M. Micheloni, P. Paoli, R. Pontellini and P. Rossi, *Inorg. Chem.*, 2006, **45**, 304–314; (*b*) M. Micheloni, M. Formica, V. Fusi, P. Romani, R. Pontellini, P. Dapporto, P. Paoli, P. Rossi and B. Valtancoli, *Eur. J. Inorg. Chem.*, 2000, 51–57; (*c*) P. Dapporto, M. Formica, V. Fusi, L. Giorgi, M. Micheloni, R. Pontellini, P. Paoli and P. Rossi, *Eur. J. Inorg. Chem.*, 2001, 1763–1774.

27 E. H. Wong, G. R. Weisman, D. C. Hill, D. P. Reed, M. E. Rogers, J. S. Condon, M. A. Fagan, J. C. Calabrese, K.-C. Lam, I. A. Guzei and A. L. Rheingold, *J. Am. Chem. Soc.*, 2000, **122**, 10561–10572 .

28 L. Broge, U. Pretzmann, N. Jensen, I. Søtofte, C. E. Olsen and J. Springborg, *Inorg. Chem.*, 2001, **40**, 2323–2334.

29 C. A. Boswell, C. A. S. Regino, K. E. Baidoo, K. J. Wong, A. Bumb, H. Xu, D. E. Milenic, J. A. Kelley, C. C. Lai and M. W. Brechbiel, *Bioconjugate Chem.*, 2008, **19**, 1476–1484.

30 N. Di Bartolo, A. M. Sargeson and S. V. Smith;, *Org. Biomol. Chem.*, 2006, **4**, 3350–3357.

31 (*a*) A. Jana, J. S. Kim, H. S. Jung and P. K. Bharadwaj, *Chem. Commun.*, 2009, 4417–4419; (*b*) A. Jana, S. Y. Jang, J.-Y. Shin, A. Kumar De, D. Goswami, D. Kim and P. K. Bharadwaj, *Chem.–Eur. J.*, 2008, **14**, 10628–10638; (*c*) K. K. Sadhu, S. Banerjee, A. Datta and P. K. Bharadwaj, *Chem. Commun.*, 2009, 4982–4984.

32 (*a*) J. C. Chambron and M. Meyer, *Chem. Soc. Rev.*, 2009, **38**, 1663–1673, and references therein; (*b*) M. Formica, V. Fusi, M. Micheloni, R. Pontellini and P. Romani, *Coord. Chem. Rev.*, 1999, **184**, 347–363; (*c*) A. Bencini, A. Bianchi, E. Garcia-España, M. Micheloni and J. A. Ramirez, *Coord. Chem. Rev.*, 1999, **188**, 97–156.

33 F. Chaux, F. Denat, E. Espinosa and R. Guilard, *Chem. Commun.*, 2006, 5054–5056.

34 (*a*) J. Dale, *Acta Chem. Scand.*, 1973, **27**, 1115–1129; (*b*) J. Dale, *Isr. J. Chem.*, 1980, **20**, 3–11.

35 K. Kumar, M. F. Tweedle, M. F. Malley and J. Z. Gougoutas, *Inorg. Chem.*, 1995, **34**, 6472–6480, and references therein.

36 A. Bencini, V. Fusi, C. Giorgi, M. Micheloni, N. Nardi and B. Valtancoli, *J. Chem. Soc., Perkin Trans. 2*, 1996, 2297–2302.

37 CrysAlis CCD, Oxford Diffraction Ltd., Version 1.171.32.5, 2008.

38 CrysAlis Red, Oxford Diffraction Ltd., Version 1.171.32.5, 2008.

39 M. C. Burla, R. Caliandro, M. Camalli, B. Carrozzini, G. L. Cascarano, L. De Caro, C. Giacovazzo, G. Polidori and R. Spagna, *J. Appl. Crystallogr.*, 2005, **38**, 381–388.

40 G. M. Scheldrick, *SHELXL-97*, Göttingen, 1997.

41 P. Gans, A. Sabatini and V. Vacca, *Talanta*, 1996, **43**, 1739–1753.